



**HAL**  
open science

# Interaction of industrial graphene and carbon nanotubes with human primary macrophages: Assessment of nanotoxicity and immune responses

Álvaro Artiga, Hazel Lin, Alberto Bianco

## ► To cite this version:

Álvaro Artiga, Hazel Lin, Alberto Bianco. Interaction of industrial graphene and carbon nanotubes with human primary macrophages: Assessment of nanotoxicity and immune responses. *Carbon*, 2024, 223, pp.119024. 10.1016/j.carbon.2024.119024 . hal-04659643

**HAL Id: hal-04659643**

**<https://hal.science/hal-04659643>**

Submitted on 23 Jul 2024

**HAL** is a multi-disciplinary open access archive for the deposit and dissemination of scientific research documents, whether they are published or not. The documents may come from teaching and research institutions in France or abroad, or from public or private research centers.

L'archive ouverte pluridisciplinaire **HAL**, est destinée au dépôt et à la diffusion de documents scientifiques de niveau recherche, publiés ou non, émanant des établissements d'enseignement et de recherche français ou étrangers, des laboratoires publics ou privés.

# Interaction of industrial graphene and carbon nanotubes with human primary macrophages: assessment of nanotoxicity and immune responses

Álvaro Artiga, Hazel Lin, and Alberto Bianco\*

CNRS, Immunology, Immunopathology and Therapeutic Chemistry, UPR3572, University of Strasbourg, ISIS, 67000 Strasbourg, France

[a.bianco@ibmc-cnrs.unistra.fr](mailto:a.bianco@ibmc-cnrs.unistra.fr)

## Keywords

Carbon nanomaterial, toxicology, immunology, macrophages, cytokines, inflammation, phagocytosis, nanosafety

## Abstract

The use of graphene and carbon nanotubes as part of commercial products has already been implemented in a wide variety of industrial sectors thanks to their outstanding physicochemical properties, opening the door to possible occupational and consumer exposure. Macrophages hold major importance in phagocytosis and immune activation against nanomaterials, so human primary macrophages are the most appropriate human models to obtain adequate information about health effects of nanomaterials. In this study, different types of industrially-employed graphene and carbon nanotubes were compared, to understand how their physicochemical properties affect cell behaviour using primary macrophages extracted from human blood donors. The phagocytic profiles were correlated with the toxicity effects provoked in the macrophages, looking to cell viability, membrane disruption and production of reactive oxygen species. To understand how these commercial nanomaterials could affect immune responses, this work was completed with a comprehensive study involving the activation of macrophages after interaction with the nanomaterials. This study provides conclusive results about the activated macrophage phenotypes and cytokine production profiles, including how the nanomaterials affect the communication of macrophages with the rest of immune cells and providing new insights about how the immune system is able to degrade these carbon-based nanomaterials.

## **1. Introduction**

The interest and importance of carbon-based nanomaterials has increased exponentially during the last decades. The use of graphene and carbon nanotubes for industrial applications has already been implemented in a wide variety of industrial sectors thanks to their remarkable physicochemical properties and multiple applications.<sup>1,2</sup> However, the employment of these nanomaterials as part of commercial products opens the door for the possibility of occupational exposure and consumer exposure.<sup>3,4</sup> For this reason, obtaining adequate information about the health effects of these nanomaterials in appropriate human models is of great importance.

Macrophages, as one of the most important cells involved in the mononuclear phagocytic system (MPS), pose major importance in phagocytosis and immune activation against exogenous agents, including nanomaterials, acting as one of the first barriers after exposure in many human tissues.<sup>5</sup> In agreement, macrophages represent one the most relevant human models to predict and understand the possible effects of nanomaterials in human health.

Although few studies have previously focused on the possible effects of graphene or carbon nanotubes in macrophages, the diversity on the experimental conditions and macrophage models employed, and the low number of comparative studies involving different types of graphene and carbon nanotubes make it difficult to extract general conclusions. Between the different commonly employed macrophage models, the majority of these studies were performed in murine macrophages<sup>6-9</sup> or immortalized macrophage cell lines.<sup>10-13</sup> It has been extensively reviewed how the immune system differs between mice and humans,<sup>14</sup> and how gene expression levels varies significantly between immortalized cell lines and healthy actual cells,<sup>15</sup> revealing both as not highly-realistic models in contrast to the primary cell model, one of the most true-to-life models.<sup>15</sup> The use of human primary macrophages obtained directly from healthy donors for carbon nanotoxicity studies is scarce.<sup>16-18</sup> However, it currently represents the most convenient and realistic human macrophage model.

Even though the usage of human primary macrophages is not usual for general toxicity experiments, the employment of nanomaterials industrially used for commercial products already available in the market is highly unusual. Most of these studies are performed with graphene and carbon nanotubes produced for research purposes, even if the real human exposure risk of these samples is extremely low in these cases. In contrast, limited studies have been performed to date with graphene or carbon nanotubes employed in

commercial products available in the market, whose exposure is generally occurring daily for workers and consumers. In addition, endotoxin has been described as a common contaminant in nanomaterial samples, which strongly affects and modulates the immunological response provoked by the nanomaterials, distorting the results obtained specially related to macrophage activation and cytokine production.<sup>19</sup> However, the number of studies which tested the presence of endotoxin on the studied nanomaterials is only a small fraction of what is available in the literature.<sup>16</sup>

One of the main goals of this study consisted on shedding light on these important aspects of nanotoxicity. In this work, different types of industrially-employed graphene and carbon nanotubes have been selected to assess their impact.. After a careful physicochemical characterization of the nanomaterials, they were dispersed by a standardized protocol to ensure uniform dispersion and comparable results. The interaction with macrophages was performed in human primary macrophages derived from monocytes and extracted from blood donors, ensuring the fidelity and reliability of the results. Using these cells, several studies were performed to test the toxicity associated with these nanomaterials, including membrane damage and oxidative stress, along with the characterization of nanomaterial phagocytosis. Macrophage activation and cytokine secretion assays were carried out to understand the inflammatory and immunologically-related responses in order to predict possible exposure outcomes. Even if a profuse phagocytosis was detected for both nanomaterials, carbon nanotubes evidenced a significant oxidative stress, while all tested graphene nanomaterials caused an increase of cytokine IL-8 expression. This study not only analyzes the potential of macrophage effects of these nanomaterials, but it also paves the way for future standardization of macrophage-nanomaterial studies and extracts insights about their possible biodegradation mechanisms.

## **2. Materials and methods**

### *2.1. Characterization of carbon nanomaterials*

Industrially employed graphene nanoplatelets and carbon nanotubes were kindly provided by the companies Creative Nano, Graphene-XT and OCSiAl Europe Sarl in the framework of the DIAGONAL European project. Graphene nanoplatelets provided by Creative Nano (GCN) are commercially available (av-PLAT-7, Avanzare). Graphene-XT provided two different samples. GXTs sample is composed of commercially available graphene nanoplatelets xGnP® grade C-500 (XG Sciences), while GXTm sample is a

mixture 1/1 in weight of xGnP® grade M-15 (XG Sciences) and GXNAN Pellet/Powder (Nanasa). Single-walled carbon nanotubes (SWCNTs) were provided by OCSiAl company, commercially available as TUBALL™. Thermogravimetric analysis (TGA) was performed on a STARE TGA 1 (Mettler Toledo) instrument with a ramp of 10 °C/min from 30 °C to 900 °C, under N<sub>2</sub> flow rate at 50 mL/min and samples deposited on platinum pans. X-ray photoelectron spectroscopy (XPS) analysis was performed on a Thermo Scientific KAlpha X-ray photoelectron spectrometer with a basic chamber pressure of 10<sup>-8</sup>-10<sup>-9</sup> bar and an Al anode as the X-ray source (1486 eV). The samples were analysed three times as powder, with a spot size of 400 µm, the survey spectra were collected as an average of 10 scans with a pass energy of 200 eV, with a step size of 1 eV and a flood gun turned on during analysis. A Quanta 250 FEG (FEI) equipped with a retractable scanning transmission electron microscopy (STEM) detector was employed for the electron microscopy observation of the dispersed nanomaterials working at a voltage of 30 KeV in STEM mode. The hydrodynamic diameter and polydispersity index (PDI) of dispersed nanomaterials were determined by dynamic light scattering (DLS) analysis using a Zetasizer Lab DLS instrument (Malvern Panalytical). Samples were diluted at 0.1 mg/mL concentration in Milli-Q® water or complemented RPMI (cRPMI), DLS measurements were performed at 25 °C and data were represented in intensity. ζ-potential was measured in similar conditions in Milli-Q water.

## *2.2. Dispersion of carbon nanomaterials*

For the dispersion of graphene samples, the standard operation procedure (SOP) corresponding to a generic dispersion protocol developed under EU NANOGENOTOX Joint Action,<sup>20</sup> was employed. Briefly, 30 µL of EtOH were added to 15.36 mg of each nanomaterial prior to the addition of 5.97 mL of bovine serum albumin (BSA) (Millipore, ref. 126579-10GM) aqueous solution at 0.5 mg/mL. The suspensions were sonicated in scintillation vials inside an ice bath by probe sonication for a total energy delivery of 7053 J, in our case using a previously calibrated sonicator VC 505 (Sonics & Materials) with a probe of 6 mm for 11 min and 15 s at an operation amplitude of 20 %. Prior to macrophage addition, the nanomaterials were freshly dispersed. Endotoxin-free BSA was filtered employing a 0.2 µm just after dispersion in water to avoid contamination or endotoxin-related problems. For the dispersion of the carbon nanotubes, it was necessary to modify the NANOGENOTOX SOP by changing the BSA dispersing agent by Pluronic F-127 (Sigma-Aldrich, ref. P2443) at 2 mg/mL and dispersing the nanomaterial at a final

concentration of 1 mg/mL without the need of pre-wetting with EtOH. The endotoxin quantification of the dispersed nanomaterials was carried out according to manufacturer instructions employing the CHROMO-LAL kit (Associates of Cape Cod, ref. C0031-5).

### *2.3. Isolation and Differentiation of PBMC-Derived Monocytes to Macrophages*

Human peripheral blood monocytes were isolated from buffy coats obtained from the French Blood Bank (Etablissement Français du Sang, Strasbourg, France, contract no. ALC/PIL/DIR/AJR/FO/606). The blood samples were from anonymous healthy donors and they do not require ethical approval. CD14<sup>+</sup> cells were isolated from healthy donor PBMCs using a positive selection kit (Miltenyi Biotech, ref. 130-050-201) and differentiated to macrophages using 40 ng/mL of M-CSF (Biolegend, #574804) for 5 days with refreshment of the cell culture medium at day 2-3. Unless otherwise stated,  $1 \times 10^5$  macrophages/well in 96 well plates were employed for most of the macrophage-related experiments. Cells were treated with 100  $\mu$ L of the nanomaterials diluted in cRPMI or with the controls for 24 h on day 5 and analysed on day 6. Cells were cultured in cRPMI (Lonza) supplemented with 10% heat-inactivated fetal bovine serum (FBS) and 1% penicillin/streptomycin at 37 °C with 5% CO<sub>2</sub>. To estimate the concentration of nanomaterials interacting with the cells, light absorbance measurements of the cells incubated with the nanomaterials or of nanomaterials in cell culture medium were collected using a Varioskan LUX (ThermoFisher Scientific) plate reader at 500-800 nm. To this end, the absorbance spectra of different concentrations of each nanomaterials were measured in the cell culture medium to produce calibration curves at 500, 600, 700 and 800 nm. After that, the absorbance spectra of the nanomaterials internalized by the cells were measured, interpolating their absorbance at 500, 600, 700 and 800 nm with the corresponding calibration curve to increase the accuracy of the measurement. All experiments with macrophages conducted in this study were performed in triplicate and analysing independently the responses produced in macrophages extracted from at least 3 different blood donors.

### *2.4. LDH release assay*

LDH release was analyzed employing the kit CytoTox 96 Non-Radioactive Cytotoxicity Assay (Promega, ref. G1781) according to manufacturer instructions. Briefly, 50  $\mu$ L/well

of culture supernatants from the treated macrophages were collected and mixed with 50  $\mu\text{L}$  of the Cytotox reagent of the kit in a new 96 well-plate. After light-protected incubation of 30 min at room temperature, 50  $\mu\text{L}$  of stop solution (1 M acetic acid) was added and absorbance at 490 nm was measured using a Varioskan LUX (ThermoFisher Scientific) plate reader. Positive controls of released LDH were treated with 15  $\mu\text{L}$  of lysis buffer (included in the kit) for 45 min at 37 °C before starting the protocol.

### *2.5. ATP content viability assay*

Viability of the cells was determined by quantifying the ATP content by the employment of CellTiter-Glo 2.0 Assay (Promega, ref. G9242). Nanomaterial-treated macrophages were washed with 100  $\mu\text{L}$  of PBS and 100  $\mu\text{L}$  of cRPMI were added. Fifty  $\mu\text{L}$  of CellTiter-Glo 2.0 reagent were added and the plate was orbitally shaken for 2 min. After 10 min incubation at room temperature, luminescence was recorded for an integration time of 1 s on a Varioskan LUX plate reader (ThermoFisher Scientific).

### *2.6. Reactive oxygen species (ROS) production quantification assay*

Nanomaterial-treated macrophages were washed with 100  $\mu\text{L}$ /well of PBS and the macrophages were incubated with 100  $\mu\text{L}$  of 10  $\mu\text{M}$  CM-H2DCFDA (ThermoFisher Scientific, ref. C6827) in PBS for 30 min at 37 °C. Samples were washed with 100  $\mu\text{L}$ /well of PBS and 100  $\mu\text{L}$  of cRPMI were added. Fluorescence emission was recorded using an excitation wavelength of 495 nm and an emission wavelength of 527 nm in a Varioskan LUX (ThermoFisher Scientific) plate reader. Positive controls were treated with 100  $\mu\text{M}$  of  $\text{H}_2\text{O}_2$ .

### *2.7. Electron microscopy visualization of the macrophages*

For TEM imaging, macrophages were cultured in 24-well plates over glass slides at a density of  $6 \times 10^5$  cells per well and exposed to 600  $\mu\text{L}$  of nanomaterials at 50  $\mu\text{g}/\text{mL}$  in completed RPMI for 24 h along with control untreated cells. Then, macrophages were washed with PBS and twice with cacodylate buffer. The fixation in 2.5 % glutaraldehyde in cacodylate buffer was performed at 4 °C overnight, followed by rinsing thrice with cacodylate buffer. Macrophages were post-fixed with 0.5% osmium tetroxide in water for 1 h at room temperature and washed thrice with Milli-Q water. Macrophages were then dehydrated through a series of ethanol baths: 25% ethanol for 10 min, 50% ethanol

for 10 min, 70% ethanol for 10 min, 95% ethanol for 15 min and 3×100% ethanol for 15 min. After that, macrophages were soaked in 1:1 ratio of 100% ethanol and Epon overnight at 4 °C. The day after, the cells were rinsed with Epon for 4 h. Final inclusion of Epon into the cells was done by polymerizing Epon at 60 °C for 48 h. Afterward, the polymerized blocks containing the macrophages were sliced into ultrathin sections of 80 nm of thickness using a diamond knife attached to a ultramicrotome cutter (Leica EM UC6). Each of the ultrathin sections were then collected on copper grids, stained with 1% uranyl acetate for 5 min followed with lead citrate staining for 2 min. Finally, the macrophage ultrathin sections of 80 nm thickness were examined by TEM at 80 kV (Hitachi H7500, Hitachi High Technologies Corporation) equipped with an AMT Hamamatsu digital camera (Hamamatsu Photonics).

### *2.8. Macrophage activation assays*

Activation of the macrophages were assessed using flow cytometry (Beckman Coulter Gallios). Control (untreated) and nanomaterial-treated cells were washed with 100 µL of PBS and cells were detached by pipetting PBS with 2% FBS and 2 mM EDTA. Positive controls of M1 activation were incubated with LPS at 10 ng/mL and for M2 activation with 20 ng/mL IL-4 (Peprotech, #200-04) and 20 ng/mL IL-13 (Biolegend, #571102) for 24 h prior to analysis. The cells were washed with 2% FBS in PBS and stained with the respective antibody at 1:50 dilution in 2% FBS in PBS at room temperature for 15 min. The anti-human antibodies used were CD14-FITC (BD Pharmingen, ref. 555397), CD86-FITC (BD Pharmingen, ref. 555657) and CD206-FITC (BD Pharmingen, ref. 551135). After staining, cells were washed with FACS buffer, resuspended in FACS buffer and analyzed by a flow cytometer.

### *2.9. Cytokines secretion analysis*

Secretion of the cytokines IL-1 $\beta$  (BD Opt-EIA #557953), TNF (BD Opt-EIA #555212), IL-6 (BD Opt-EIA #555220), IL-8 (BD Opt-EIA #555244), IL-10 (BD Opt-EIA #555157) and IL-12 (BD Opt-EIA #555183) were assessed by ELISA kits according to the manufacturer's instructions. Briefly, polyvinyl microtiter 96-well plates (Falcon) were coated overnight at 4 °C with 50 µL/well of purified capture antibodies diluted in coating buffer (carbonate/bicarbonate buffer 0.05 m, pH 9.6). After washing with PBS

containing 0.05% Tween (PBS-T) for 3 times, a blocking step was performed by adding 2% FBS in PBS (50  $\mu$ L per well) for 1 h at room temperature. After washing thrice with PBS-T, 50  $\mu$ L of a respective series of standards dilutions provided in the kits or 50  $\mu$ L of culture supernatants from the treated macrophages were added in the respective wells. The plates were incubated at room temperature for 2 h and washed thrice with PBS-T. Secondary antibodies and horseradish peroxidase provided in the kit were then added together and incubated for 1 h at room temperature. Then, the plates were washed five times with PBS-T and the detection reaction was started by adding tetramethylbenzidine in the presence of H<sub>2</sub>O<sub>2</sub>. The reaction was stopped after 15 min at room temperature by the addition of 2 N HCl and the resulting absorbance was measured at 450 nm in a Varioskan LUX (ThermoFisher Scientific) plate reader.

### 2.10. *Statistical Analysis*

Experiments were conducted at least three times with macrophages obtained from different blood donors and results were expressed as mean  $\pm$  standard deviations. Statistical analysis was processed using GraphPad Prism 8 software and one-way ANOVA followed by Bonferroni's test was performed to determine the statistical differences among samples versus control untreated cells (\* $p \leq 0.05$ ; \*\* $p \leq 0.005$ , \*\*\* $p \leq 0.0005$ ).

## 3. **Results and discussion**

### 3.1. *Physicochemical properties of the nanomaterials*

The physicochemical properties of carbon nanomaterials determine their impact in a biological context. Properties such as size, thickness, surface composition and shape control the interaction with the rest of biological environment components, govern the protein corona formation and the cellular interaction and internalization, determining the toxicity profiles and the immune response. In this study, different industrially employed carbon nanomaterials with different shapes, sizes and compositions, employed in a wide variety of applications, were selected for their comparison in terms of macrophage interaction, nanotoxicity and immune response (**Figure 1**). GCN graphene is employed by Creative Nano company to produce anticorrosion composite coatings of metal matrixes, with industrial application in automotive and oil and gas tanks. GCN is in the form of nanoplatelets showing a lateral size of 7.2  $\mu$ m, a thickness of 12 nm composed by a multi-layered structure with an average number of 40 layers (**Figure S1**) and a

Brunauer–Emmett–Teller (BET) surface area of 70 m<sup>2</sup>/g, according to suppliers. GXTs and GXTm are employed by Graphene-XT to produce textiles with electrical and thermal properties and reinforced coating formulations for paints. GXTs graphene nanoplatelets possess a particle lateral size below 2 μm, thickness of few nm (**Figure S2**) and a BET surface area of 500 m<sup>2</sup>/g, while GXTm sample was composed of a mixture of graphene sheets of 15 μm, with 6-8 nm thickness (**Figure S3**) and surface area 120-150 m<sup>2</sup>/g. SWCNTs are utilized by OCSiAl as ingredient in an epoxy floor additive for industrial floor coatings in order to take advantage of their antistatic and mechanical properties. These single-walled carbon nanotubes are produced with a diameter of 1.6±0.4 nm, approximately 5 μm length (**Figure S4**), a BET surface area between 300 and 700 m<sup>2</sup>/g and they can contain until 10-15% of iron nanoparticles inside the carbon nanotubes due to the fabrication process according to the manufacturer.

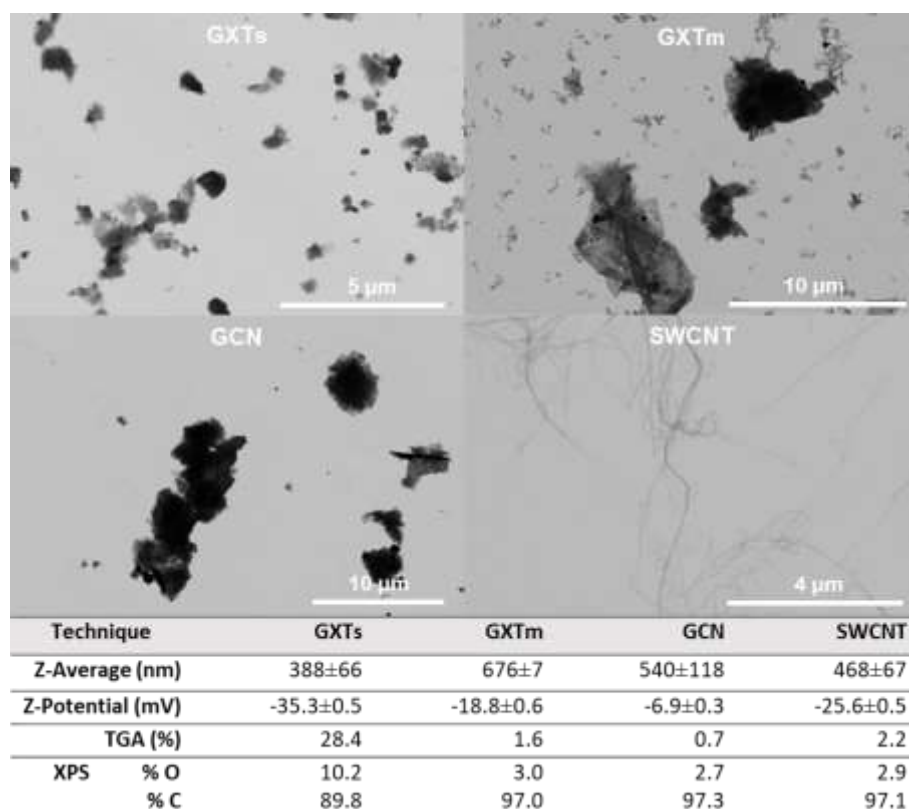


**Figure 1.** Physicochemical characterization of the carbon nanomaterials employed in the study: GXTs, GXTm, GCN and SWCNTs. Top panels, STEM images of the nanomaterials after their dispersion employing NANOGENOTOX protocol. Bottom table, Z-Average size measured by DLS after nanomaterial dispersion and Z-Potential, % of weight loss at 700 °C using TGA and XPS elemental quantification.

The different nanomaterials were also analyzed by TGA (**Figure 1** and **Figure S5**). Almost no mass loss (<2.2%) was measured during the analysis of GCN, GXTm and SWCNTs, indicating the absence of organic components or functional groups in their structure. GXTs showed instead an unexpected loss of mass of about 28% starting at 300 °C indicative of the presence of some functional groups or organic compounds in this sample.

As the surface composition of a nanomaterial or a nanoparticle determines the protein corona formation and their interaction with the cellular membranes,<sup>5</sup> the surface characterization was of great importance in this study. Using XPS, it was possible to determine the atomic percentage in the surface of the nanomaterials (**Figure 1** and **Figure S6**). No other atomic elements than carbon and oxygen were detected in concentrations beyond the limit of detection of the technique in any of the samples. As expected, C appeared as the major element in all the samples, while O was found in low percentages in CGN, GXTm and SWCNTs, indicating almost any degree of oxidation of the samples. However, GXTs showed a 10.2 % of O, indicating a higher degree of oxidation or organic groups on its surface, in agreement with TGA result.

To properly evaluate the nanomaterial-biological interaction in aqueous environments, it is necessary that the nanomaterial remains colloidally dispersed, since non-dispersed nanomaterials will behave as macroscale materials without interactions at the cellular scale.<sup>21</sup> For this reason, the dispersion of the nanomaterials is a crucial parameter for their hazard assessment, which is not always taken into consideration. The wide range of dispersing agents and dispersing methodologies employed in the literature complicate severely their comparison in the nanosafety field. In this context, we would like to encourage the employment of standardized dispersion protocols for hazard assessment. For this study a standard operation procedure (SOP) for nanomaterial dispersion developed under EU NANOGENOTOX Joint Action, based on BSA as dispersing agent and probe sonication, was adopted for the dispersion of GXTs, GXTm and GCN. However, SWCNTs remained particularly difficult to disperse and this protocol was not efficient to obtain a homogeneous colloidal dispersion. Although the risk of exposure to SWCNT in aqueous media is extremely low, there are other exposure routes such as dermal exposure or inhalation where carbon nanotubes can interact as nanoforms with cells and macrophages.<sup>22</sup> For this reason, the standard dispersion protocol was adapted employing Pluronic F-127 to have the opportunity to study macrophage-carbon nanotube interaction.

DLS is commonly employed as the gold standard technique to analyse dispersion of nanoparticles and nanomaterials.<sup>23</sup> DLS was employed to analyze the nanomaterial dispersion degree after their suspension on BSA/water and in cell culture medium determining the Z-average size according to ISO22412:2008 (**Figure 1**, **Figure S7** and **Figure S8**). We would like to underline that it has to be taken into account that DLS is a technique designed to measure the size of spherical particles with a monodisperse distribution and with a total colloidal stability. When one of these conditions are not fulfilled, the equipment registers the scattering pattern of the sample and tries to model it to the scattering of a perfectly dispersed spherical particle.<sup>24</sup> For this reason, the size provided by the equipment is the hydrodynamic diameter of a spherical nanoparticle with a scattering patterning similar to the one measured for the sample. In conclusion, it is not possible to precisely measure the size of 2D or rod-like nanomaterials and the DLS size obtained would be something intermediate between the largest and shortest dimensions. However, this technique is highly useful to estimate the dispersion of anisotropic nanomaterials and in all the cases the nanomaterials employed in this study showed a Z-average size below the sub-micron scale, enough dispersed for cellular studies. As expected, the Z-average size of the four nanomaterials studied showed an intermediate value (from 380 nm to 680 nm) between the largest dimension (several microns) and the shortest dimension (few nm) observed in the STEM images. The surface charge was also analyzed after the dispersion of the nanomaterials (**Figure 1**), showing a negative Z-potential (from -7 to -35 mV) in the four cases as expected.

As previously mentioned, endotoxin strongly affects and modulates the immunological response provoked by the nanomaterials,<sup>19</sup> although its presence is not sufficiently analyzed in an important portion of the available studies, misrepresenting their results. To ensure that endotoxin levels were not affecting our study, an endotoxin LAL assay previously employed to ensure endotoxin-free carbon nanotubes<sup>18</sup> was employed to prove the absence of endotoxin in our study. In this line, we found particularly important to employ endotoxin-free BSA in sterile conditions for the dispersion protocol to avoid bacteria proliferation and endotoxin contamination of the samples. When endotoxin-free BSA in sterile conditions was employed, the endotoxin levels of the four nanomaterials studied remained below the limit of detection.

### *3.2. Macrophage cytotoxicity, membrane integrity and cell stress*

After ensuring the absence of undesired endotoxins in the tested nanomaterials and their proper dispersion, a study was carried out to analyze the basal cytotoxicity associated with the four types of carbon nanomaterials. Human primary macrophages obtained from blood donors<sup>17</sup> were exposed to the nanomaterials at different concentrations (10, 25, 50 and 100  $\mu\text{g}/\text{mL}$ ) for 24 h and the ATP content was determined to evaluate the viability of the cells (**Figure 2A**). No signs of toxicity were detected for any of the graphene samples or for the dispersing agents BSA and Pluronic F127 (Plur 127). However, a slight but non-significant decrease of viability was observed for the carbon nanotubes at 50  $\mu\text{g}/\text{mL}$  and a significant decrease of 26 % when exposed to SWCNTs at 100  $\mu\text{g}/\text{mL}$  in comparison with untreated cells, proving a certain degree of cytotoxicity associated to carbon nanotubes at higher doses. It is noteworthy that ATP content assay was compared in preliminary studies with MTS assay and other commonly employed fluorescent techniques for viability determination (data not shown) and that ATP content assay showed the most consistent results without interferences related to carbon nanomaterials thanks to the employment of luminescence for the quantification instead of absorbance or fluorescence. For these reasons, we would like to suggest this technique as a complementary additional alternative for the standardization of viability measurements concerning carbon-based nanomaterials or other nanomaterials with strong optical absorption properties. The results obtained with ATP content determination were consistent with complementary measurements using Fixable Viability Dye eFluor® 450 during flow cytometry analysis (data not shown).

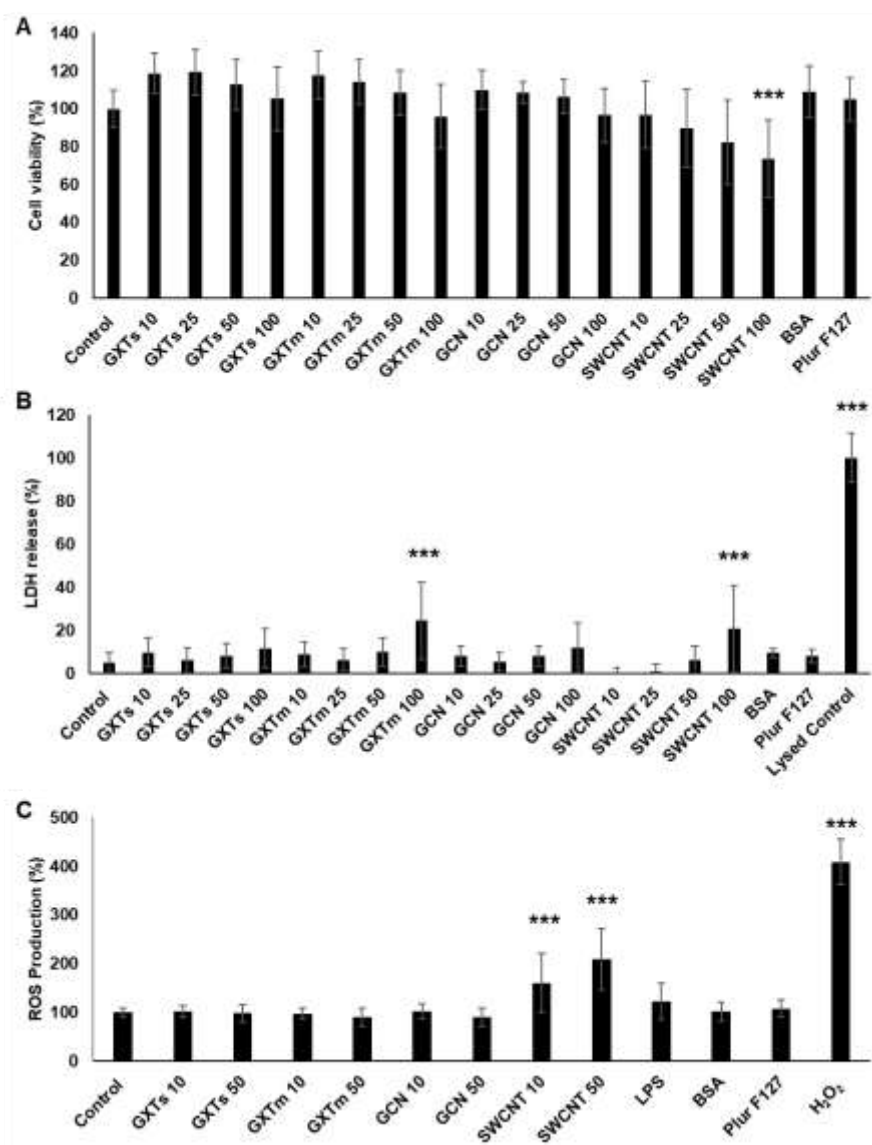


**Figure 2.** A) ATP content viability assay results of the macrophages after incubation for 24 h with the nanomaterial samples: GXTs, GXTm, GCN and SWCNT at different concentrations (10, 25, 50 and 100  $\mu\text{g}/\text{mL}$ ) and with the dispersant agents at the highest concentration employed. B) LDH release assay results of the macrophages after incubation for 24 h with the nanomaterials including a positive control of the untreated macrophages artificially lysed. C) ROS quantification assay of the macrophages after incubation for 24 h with the nanomaterials at different concentrations (10 and 50  $\mu\text{g}/\text{mL}$ ) including a positive control of the untreated macrophages exposed to 100  $\mu\text{M}$  of  $\text{H}_2\text{O}_2$ .

In order to complement the previous results, LDH release assay was employed to determine the cytoplasmic membrane disruption as a sign of toxicity and/or damage caused to the cells (**Figure 2B**). This test has been proposed as one of the gold standards in cell cytotoxicity assessment.<sup>25</sup> The tendency of LDH results was aligned with ATP

content, with non-significant slight increase of LDH release for GXTs and GCN at 100  $\mu\text{g}/\text{mL}$  and a clear membrane disruption for GXTm (24 %) and SWCNTs (21 %) in comparison with the fully lysed macrophage control. In conclusion, taking into account the ATP content study along with LDH release assay, the studied nanomaterials did not display a remarkable macrophage toxicity, and signs of toxicity were only detected for GXTm and SWCNTs at the highest doses. The importance of macrophages as the main immune cells that interact with nanomaterials along with the employment of a highly realistic model (human primary macrophages extracted for blood donors) confers great importance to the obtained results. Given the large number of commercial products incorporating CNMs and the high likelihood of consumer exposure, this issue is of paramount importance for future legislation, regulation and use.

Differences in cytotoxicity of different carbon-based nanomaterials have been attributed to the variances in size, degree of dispersion, degree of oxidation and the various cellular models applied. Although all these variables condition the toxicity assessment, these results are in agreement with previous studies reported in the literature, where multi-walled carbon nanotubes displayed LDH release at concentrations of 50-100  $\mu\text{g}/\text{mL}$  in monocyte-derived macrophages.<sup>18,26</sup> Other carbon-based nanomaterials displayed associated toxicities at 100  $\mu\text{g}/\text{mL}$  measured by other techniques such as staining with propidium iodide.<sup>17</sup>

As the different mechanisms of toxicity or death can interfere with the rest of metabolic pathways in macrophages, the rest of the present study including ROS production, phagocytosis and macrophage activation was carried out at non-toxic nanomaterial concentrations of 10 and 50  $\mu\text{g}/\text{mL}$ . The increase of ROS production was measured using CMH2DCFDA, a commercial dye derivative of H2DCFDA with improved retention in living cells, to monitor general ROS generation inside the cells. SWCNTs produced a clear increase in ROS generation, proportional to the concentration of the nanomaterial, to 160 % at 10  $\mu\text{g}/\text{mL}$  and 210 % at 50  $\mu\text{g}/\text{mL}$ . Increase of ROS production was not detected for any of the graphene samples nor the control of activation of the macrophages, namely LPS at 10 ng/mL. It is not very common to report nanomaterial-exposure ROS production, although it has been described that ROS play an important role in the activation of pro-inflammatory signaling pathways.<sup>27</sup> Between the few studies carried out, it was reported that pulmonary surfactant coated multi-walled carbon nanotubes displayed high ROS production in human primary macrophages.<sup>28</sup> However, similar to this study,

graphene oxide did not produce any significant ROS response in monocyte derived macrophages.<sup>17</sup>

### *3.3. Nanomaterial interaction with macrophages and phagocytosis*

It has been reviewed how nanomaterials can interact and be endocytosed by the cells in different manners: clathrin-mediated endocytosis, clathrin-independent/dynamin-dependent endocytosis, clathrin-independent/dynamin-independent endocytosis, micropinocytosis, and phagocytosis.<sup>29</sup> In addition, it has been extensively proven how the amount of nanomaterials that interacts with the cell is critical for their cellular effects.<sup>30,31</sup> The quantification of the nanomaterials that is internalized by the cells and the different cellular compartments in which they are accumulated have been reported as crucial parameter to determine nanomaterial associated toxicity.<sup>31,32</sup> However, most of the works in the field do not take into account these variables and it is common to find studies where the amount of nanomaterials inside the cells is not quantified or not even confirmed by any technique, extracting conclusions without any information regarding the actual presence of the nanomaterials inside the cells.

To increase the relevance of this work, we were highly interested in understanding if these nanomaterials were highly internalized by macrophages, despite their rather large size, and the amount taken up. For other types of nanomaterials like metal nanoparticles of other 2D materials made of other elements than only carbon, it is common to employ elemental analytical techniques, such as ICP-MS, to quantify the elements which are part of the nanomaterials but are not commonly found in cells (e.g., carbon, nitrogen and oxygen).<sup>31,32</sup> Nevertheless, in carbon-based nanomaterials these approaches cannot be implemented due to the major presence of C as cell component. To date, between the few studies which quantifies carbon-nanomaterials internalization, most of them employ highly complex, time-consuming and expensive techniques difficult to implement for toxicological studies. As an illustrative example, some of these elaborate strategies includes single-cell mass cytometry,<sup>33</sup> confocal Raman microscopy<sup>34</sup> and the indirect conjugation of other elements followed by ICP-MS quantification,<sup>35</sup> not easy available for most laboratories involved in nanomaterial exposure assessment.

However, thanks to the high optical contrast provided by carbon-based nanomaterials, it was easy to recognize them once they were internalized by the cells, especially in the case of the graphene samples (**Figure 3A-E**).

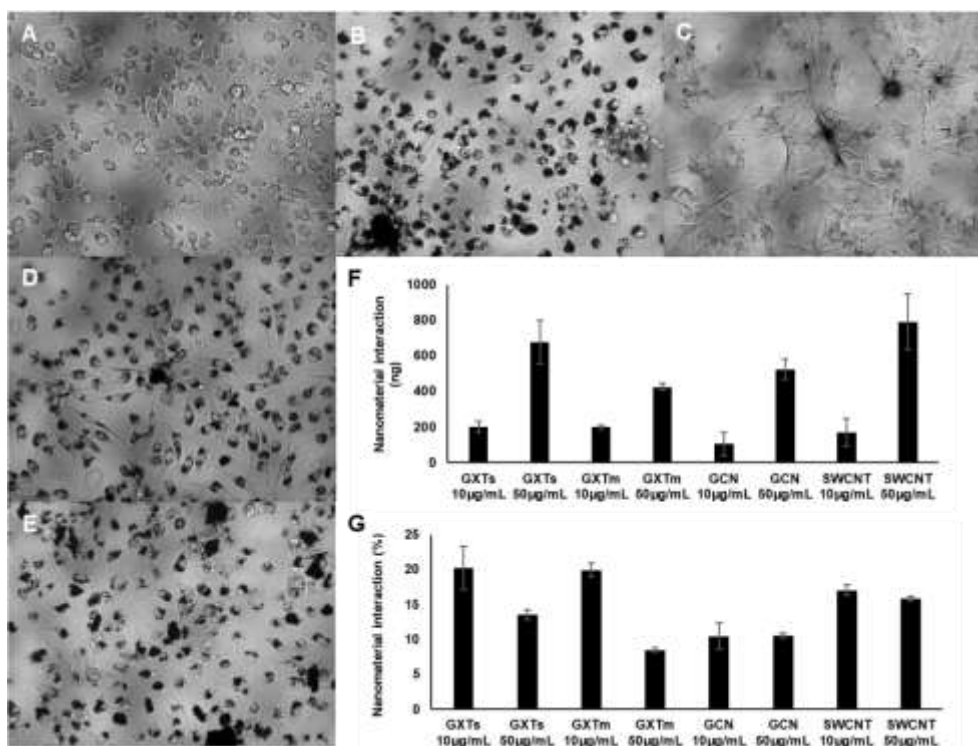


**Figure 3.** Representative optical microscopy images of the macrophages untreated (A), after incubation for 24 h with 50 µg/mL of GCN (B), SWCNTs (C), GXTs (D) or GXTm (E). Quantification of nanomaterial interaction based on visible light absorbance of the nanomaterials inside the cells after incubation (measured at 500-800 nm), according to total amount quantified (F) and as percentage of nanomaterials originally added to cells (G).

As can be observed in **Figure S9-S12**, the quantity of nanomaterials internalized and the increase of contrast on the images is proportional to the dose of nanomaterials incubated with the macrophages. This fact made us to propose a novel approach to determine the quantity of nanomaterial interacting with the macrophages based on the increase of light absorbance caused by these carbon nanomaterials. As an exploratory approach, the spectrum of light absorbance was recorded for the untreated cells and for the cells incubated with the nanomaterials after extensive washing to discard all non-internalized nanomaterials (**Figure S13**). Using the untreated cell spectrum as the blank, it was possible to extract the absorbance spectra of the nanomaterials interacting with the cells. These spectra were employed to estimate the amount of nanomaterials internalized by the cells, by correlating their absorbance intensity at 500, 600, 700 and 800 nm with a calibration curve of the same nanomaterial at known concentrations in cell culture medium. These wavelengths were selected to avoid interference with macrophages and cell culture medium components. Although light absorbance has been employed rarely

for carbon nanomaterial quantification in cells employing more complex strategies,<sup>36,37</sup> we would like to highlight that this is the first time that the absorbance has been directly measured in living cells seeded in wells without intermediate steps. Thanks to this strategy developed in this study, it was possible to easily measure the total amount of nanomaterial interacting with the macrophages (**Figure 3F**) and it was possible also to correlate the results to the initial amounts employed for the incubation to determine the percentage of the nanomaterials interacting with the macrophages (**Figure 3G**). As expected, the quantity of nanomaterials interacting with macrophages was higher for the 50  $\mu\text{g/mL}$  dose in comparison with the 10  $\mu\text{g/mL}$  dose, with ratios between 2 and 4 times higher depending on the nanomaterial (**Figure 3F**), in accordance with the nanomaterial phagocytosis observed in the optical microscopy images. When the percentage of nanomaterials interacting with the macrophages is analyzed (**Figure 3G**), it can be observed how the percentage of nanomaterial internalized was slightly slower for the higher doses, probably due to a saturation phenomenon commonly observed in dose-response curves. The percentages of the nanomaterial interaction were maintained between 10 and 20 % approximately for all cases.

Considering TEM as the gold standard technique to confirm material uptake within cells, the subsequent step was to compare the uptake of all the carbon-based nanomaterials studied. In this regard, TEM imaging revealed that the four types of nanomaterials exhibited cellular uptake by the macrophages (**Figure 4**). The high contrast produced by the nanomaterials made it easy to recognize the graphene flakes and carbon nanotubes in comparison with the low-contrast cellular structures. All materials were observed to be internalized within phagocytic vacuoles, in different amounts and in varying degrees of aggregation (**Figure 4** and **Figures S14-S18**). However, in some of the images it was not possible to elucidate if the nanomaterials were localized inside intracellular organelles or remained inside the cytoplasm of the cells. GXTs uptake was found to involve invaginations that could be attributed to either phagocytosis or endocytosis (**Figure S15**). It is noteworthy that the three types of graphene were extensively found in the majority of the macrophages, occupying broad areas in the interior of the macrophages, inside vacuoles or forming large aggregates of several microns of size. However, SWCNT aggregates were observed in lower frequencies in the images taken, likely indicating a lower internalization rate or a more difficult detection and observation in the images. This appears to be in high agreement with the previously described optical images (**Figure 3**). In the case of SWCNTs, they were found forming aggregates resembling a skein, showing

a complete bending of the nanotubes inside cellular compartments as previously described in other studies.<sup>38</sup> The strips and small holes that can be observed in some of the images were produced due to the hardness of the carbon nanomaterials aggregates, which were damaging the diamond blade employed to cut the ultrathin slices observed on the TEM and provoking the small holes in the resin embedding the cells. No apparent differences in mitochondria, in terms of distortion or damage, were observed for any of the nanomaterials, neither were double-stranded autophagosome-like organelles nor other abnormal structures identified containing the four materials.

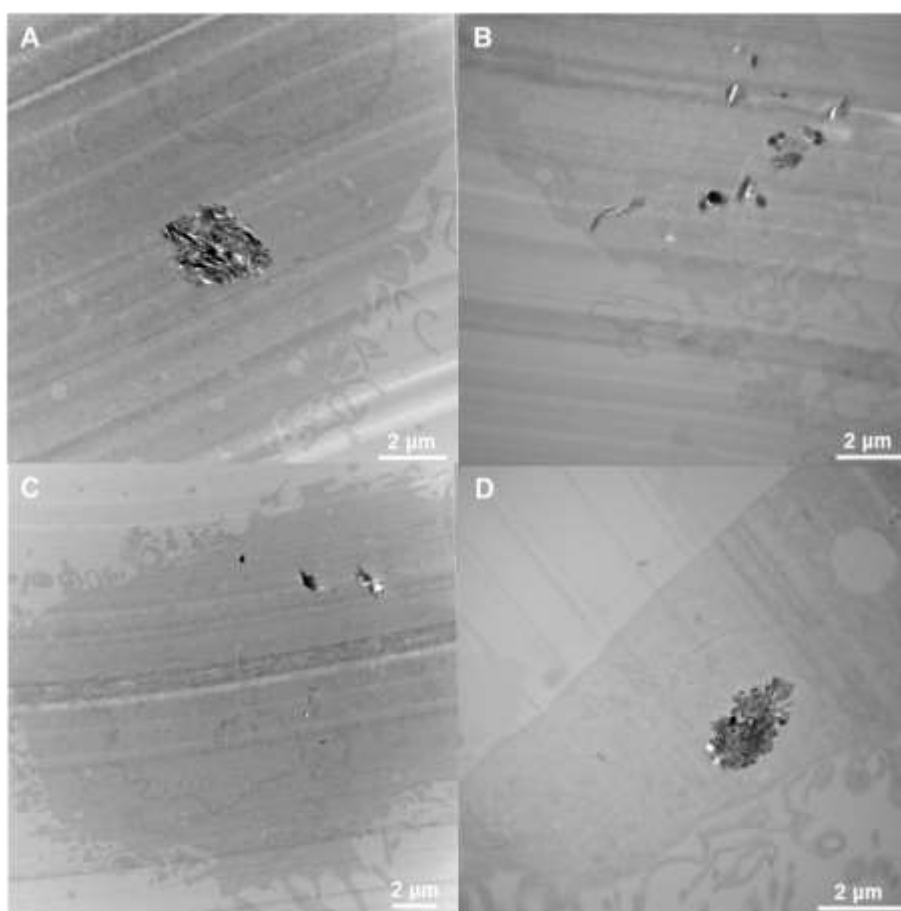


**Figure 4.** Representative transmission electron microscopy images of macrophages after incubation for 24 h with 50 µg/mL of GXTs (A), GXTm (B) GCN (C), or SWCNTs (D) showing the nanomaterials inside the macrophages.

#### 3.4. Macrophage activation and cytokine secretion

Once it was proved that 50 µg/mL remained as a nontoxic concentration for all tested nanomaterials and that all nanomaterials were internalized by the macrophages in high doses, their effect on the macrophage immune response was evaluated. In the first part of

the study, the activation of macrophages was evaluated by the expression of surface markers CD86 and CD206 (**Figure 5A** and **5B**). CD86 is a pro-inflammatory marker commonly employed to monitor the activation of M1 macrophages. The macrophages incubated with the nanomaterials were compared with untreated cells and cells incubated with 10 ng/mL LPS, one of the most potent activators of pro-inflammatory response, frequently employed as a positive control. In this study, GXTs and GCN did not display any CD86 activation change. However, the SWCNTs provoked a strong pro-inflammatory CD86 response, even at the low dose of 10 µg/mL of nanomaterial. The iron content of SWCNTs described by the manufacturer could contribute to increase the macrophage activation, as it has been described that iron nanoparticles can provoke a M1 macrophage polarization.<sup>39</sup> GXTm exhibited an intermediate CD86 expression response, showing an activity similar to LPS only when GXTm were added at 50 µg/mL. It has been previously reported that CD86 was overexpressed in human primary macrophages after their exposure to high concentrations of graphene oxide,<sup>17</sup> in concordance with our research.

In parallel, the anti-inflammatory response caused by the nanomaterials was evaluated on the basis of CD206 expression changes. CD206 represents a common marker of M2 macrophage differentiation and this response can be artificially induced by the addition of interleukins (IL) like IL-4 and IL-13, usually employed as efficient positive controls of anti-inflammatory responses. In this case, none of the nanomaterials provoked any remarkable CD206 activation, although SWCNTs at 50 µg/mL produced a slight non-significant increase of CD206 expression. It has been described before that carbon nanotubes (both SWCNTs and MWCNTs) were able to stimulate M2 polarization in murine macrophage,<sup>40</sup> however this study was carried out in M2 polarization conditions in contrast to our studies.

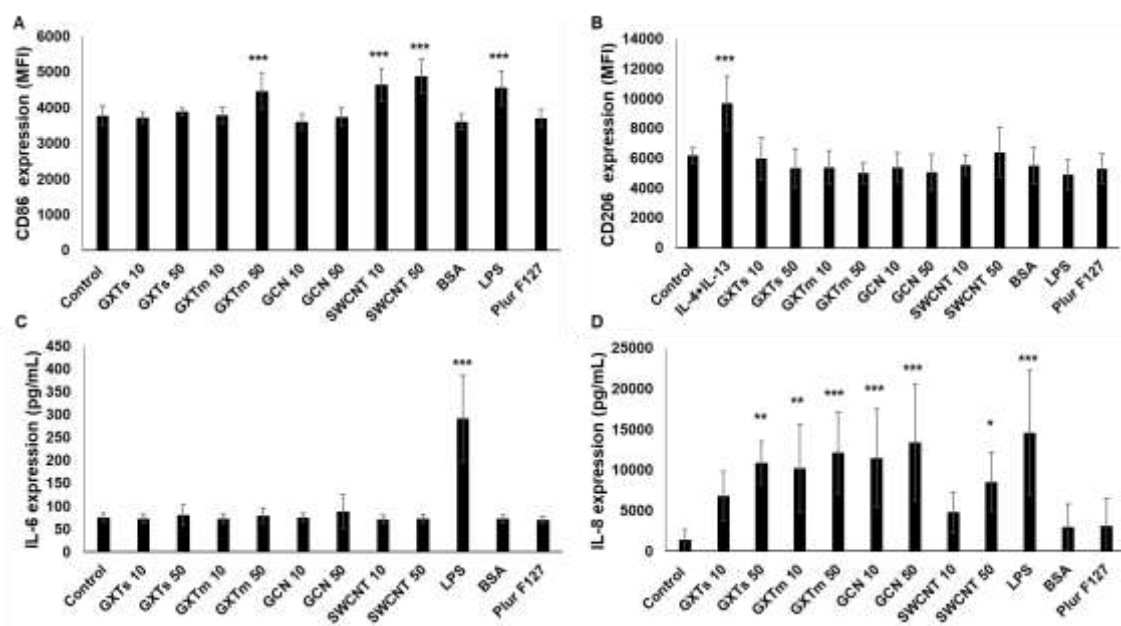


**Figure 5.** A) CD86 expression quantification by flow cytometry after incubation of macrophages with the nanomaterials at 10 or 50  $\mu\text{g/mL}$  for 24 h. B) CD206 expression quantification by flow cytometry after incubation of macrophages with the nanomaterials at 10 or 50  $\mu\text{g/mL}$  for 24 h. C) IL-6 expression quantification by ELISA after incubation of macrophages with the nanomaterials at 10 or 50  $\mu\text{g/mL}$  for 24 h. D) IL-8 expression quantification by ELISA after incubation of macrophages with the nanomaterials at 10 or 50  $\mu\text{g/mL}$  for 24 h.

Once the activation profile of the macrophages caused by the nanomaterials was analyzed, our last attention was to understand how these nanomaterials could affect the response of the macrophages to modulate the rest of the immune system. It has been proposed that macrophages are able to sense carbon nanotubes via Toll-like receptors causing the release of interleukin and other cytokines.<sup>41</sup> In order to study this issue, the production of interleukins and other cytokines was analysed after 24 h incubation with the different nanomaterials. Several cytokines commonly produced by macrophages in response to different stimuli and with different functions on the rest of the immune cells were chosen: pro-inflammatory IL-6, IL-1 $\beta$ , IL-8 and TNF- $\alpha$  and anti-inflammatory IL-10 and IL-12. In summary, no significant alterations were found for IL-6, IL-1 $\beta$ , TNF- $\alpha$ , IL-10 or IL-12 after the exposure to any of the nanomaterials (**Figure 5** and **Figure S19**). The only significant clear increase in the production of these cytokines was observed after the incubation with the positive control LPS. In detail, slight non-significant increases were observed in the case of GXTm at 50  $\mu\text{g/mL}$  for IL-10 and in the case of the three graphene samples at 50  $\mu\text{g/mL}$  for IL-12. However, these increases were negligible in comparison

with the increases produced during activation with the positive controls. These results suggest that these nanomaterials would not affect substantially crucial immune networks controlled by macrophages, such as B-cell differentiation (IL-6), phagocyte activation of macrophages (TNF- $\alpha$ ) or general pro-inflammatory response caused by IL-1 $\beta$ . They would also not affect the important pathways controlled by IL-10 and IL-12, involved in inhibition of cytokine production and activation of NK cells and phagocyte cells, respectively.

In comparison with these results, it was reported that graphene oxide was able to cause a slight production of TNF- $\alpha$  without increasing IL-1 $\beta$  or IL-6 release.<sup>17</sup> Interestingly, it has been described that human primary macrophages were less reactive to carbon nanotubes than the THP-1 macrophage cell line, displaying no cytokine production in contrast to THP-1 activated macrophages,<sup>18</sup> in agreement with our results. In concordance, graphene and carbon nanotubes did not display any release of TNF- $\alpha$ , IL-6 or IL-10 in human primary monocytes,<sup>42</sup> and graphene oxide was not producing TNF- $\alpha$  or IL-10 secretion, unless human primary macrophages were primed with LPS,<sup>16</sup> reiterating the absolute importance of endotoxin nanomaterial quantification in these studies.

However, a totally different situation occurred when the pro-inflammatory IL-8 expression was analysed. It should be highlighted that all the nanomaterials provoked a clear increase in the production and liberation of IL-8 by the macrophages in a dose-dependent manner. The response was more intense in the case of graphene samples than for the SWCNTs, and in particular the response was even more severe for the bigger graphene GXTm and GCN with IL-8 expression levels similar to LPS exposure. These results correlate with the evidences found in other simpler models, such as macrophage cell lines,<sup>11</sup> other cell lines derived from various tissues,<sup>43</sup> and *in vivo* models such as the zebrafish<sup>44</sup> and the lungs of rodents,<sup>6,45</sup> where the exposure to carbon nanotubes or graphene resulted in a significant increase production of IL-8. However, as long as we know, this study proved for the first time an increased release of IL-8 by human primary macrophages due to graphene exposure. This supports previously published data showing an increase in IL-8 secretion in THP-1 macrophages after treatment with graphene.<sup>46</sup> Interestingly, another study in primary human macrophages did not show an increase in IL-8 after GO exposure,<sup>16</sup> alluding to possible differences in macrophage response with regards to different types of nanomaterials.

To date, increased levels of IL-8 after nanomaterial exposure have been considered as signs of potential toxicity and altered immune response.<sup>6,45</sup> This conclusion remains logical as higher levels of IL-8 have been correlated with several health problems and diseases. As an illustrative example, there has been a significant association between higher levels of IL-8 during second-trimester maternal and a greater risk of schizophrenia spectrum disorders in the offspring.<sup>47</sup> However, IL-8 has also been extensively described as a potent chemotactic molecule with a key role on neutrophil attraction to the site of action and neutrophil granule-content release.<sup>48</sup> In another study, it was shown how graphene was able to activate neutrophils, provoking the release of myeloperoxidase at the same time that ROS were generated.<sup>49</sup> In parallel, our group previously reported how neutrophil myeloperoxidase was highly efficient in graphene degradation.<sup>50,51</sup> Although these findings have been described in independent studies, to date nobody has tried to interrelate them and nobody has explored the importance of IL-8 production increase in the biodegradation of carbon nanomaterials. Based on all evidences from these different studies together, we would like to propose a possible alternative mechanism for the biodegradation of carbon nanomaterials to be comprehensively studied in future (**Figure 6**). In this mechanism, macrophages and other cells would produce IL-8 in response to the nanomaterial exposure, as shown in **Figure 5D**. IL-8 would provoke neutrophil attraction to the site of action. Once neutrophils reach a threshold of exposure, their interaction with carbon nanomaterials would provoke their activation and degranulation, as described in the literature. The degranulation of neutrophils would lead to the release of myeloperoxidase. Finally, myeloperoxidase and other possible factors would play an important role in the biodegradation of these nanomaterials through their oxidation, as previously described.<sup>51,52</sup>

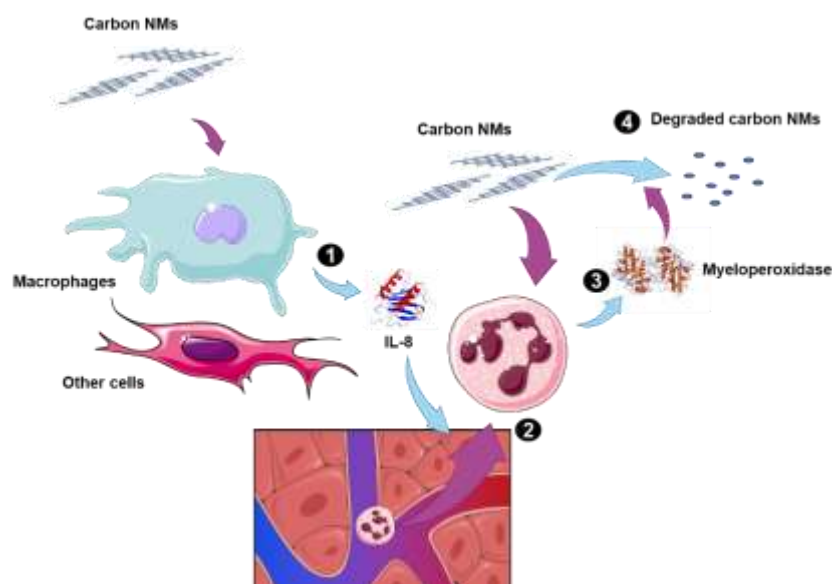


**Figure 6.** Hypothesized mechanism describing the role of IL-8 mediating carbon-nanomaterial degradation. 1) The presence of carbon nanomaterials produces the liberation of IL-8 by macrophages and other cells. 2) IL-8 has a key role in neutrophil attraction to the tissues where carbon nanomaterial exposure takes place. 3) Neutrophils secrete myeloperoxidase in the presence of carbon nanomaterials. 4) Myeloperoxidase has been described as a potent peroxidase enzyme with the capacity to degrade carbon nanomaterials.

IL-8 increase has also been described as a consequence of nanomaterial exposure during extended periods of time. 90-day chronic inhalation of carbon black nanoparticles produced a significant increase in IL-8 levels and neutrophil counts in rats.<sup>53</sup> Interestingly, coal workers' pneumoconiosis, a chronic inflammation of the lung, which occurs when coal dust is inhaled, has been correlated with increased levels of IL-8 in patients' serum.<sup>54</sup> This finding could support our proposed mechanism for carbon nanomaterial degradation in the human body or, at least, to remark the importance of IL-8 as a possible key element in these nanomaterial degradation. Probably, the proposed mechanism is not fully complete and additional steps are still to be described, e.g. eosinophil peroxidase has also been described as a possible enzyme involved in carbon nanomaterial degradation.<sup>51</sup> However, according our criteria, this mechanism and the role of IL-8 could represent a crucial starting point to completely unravel the critical issue for carbon nanomaterial regarding their human biodegradation and safety. As a conclusion, increased production of IL-8 by macrophages observed in this study could represent not only a change in the immune response but also a possible alternative process to activate the human biodegradation pathways of these nanomaterials.

#### **4. Conclusions**

Although the use of graphene and carbon nanotubes as part of commercial products has already been implemented in a wide variety of industrial sectors, there is still a clear lack of knowledge concerning risks associated with consumers and occupational exposure. The lack of realistic models along with the inconsistencies and the absence of standardization during the assessment process make it almost impossible to extract general conclusions or to predict the safety or hazard of the nanomaterial exposure.

In this work, we have improved the reliability of the employed models, testing conditions and standardization of the assessment in comparison with previous studies. Actual industrially employed carbon nanomaterials with different shapes and different physicochemical characteristics have been selected for the study along with the employment of human primary macrophages freshly extracted from blood donors, considered one of the most realistic models to study phagocytosis and immune activation against nanomaterials. The reliability and comparability of the results was also improved by the employment of standardized operation protocols for nanomaterial dispersion and endotoxin-free testing, and employment of cellular biology techniques with lower interferences caused by nanomaterials properties.

In this realistic model, it has been confirmed that the nanomaterials tested were internalized in high amounts, especially in the case of the different tested graphene samples. Despite high internalization, the cytotoxicity and membrane disruption associated with these nanomaterials was quite low, only remarkable at higher concentrations difficult (if not impossible) to achieve in real exposure scenarios. However, cell stress measured by ROS production was clearly produced by SWCNTs even at lower doses, highlighting that even if the nanomaterials are not provoking cell death, they can affect cell metabolism and cellular functions.

The most interesting and unexpected results appeared to our eyes when immune activation of the macrophages was analyzed. Although some slight pro-inflammatory differentiated macrophage profiles were provoked by GXTm and SWCNTs, common pro-inflammatory and anti-inflammatory cytokine production was absent. However, a high production of the pro-inflammatory IL-8 was detected for the four carbon

nanomaterials, providing a result never reported for graphene interaction with human primary macrophages. These findings along with other previously reported studies using other models allows us to hypothesize a link between the response provoked by carbon nanomaterials in macrophages, the neutrophil attraction and the carbon nanomaterial degradation, suggesting an important role of this interleukin in the human biological mechanism for carbon-based nanomaterial degradation. This work opens the door for additional future studies to fully prove in the future this alternative mechanism associated to IL-8 overexpression.

### **CRedit authorship contribution statement**

AA and AB planned the experiments. HL and AA optimized the protocols for human primary macrophages studies. AA carried out the experimental part. AA analyzed the data, carried out the statistical analysis and prepared tables/figures. AB searched for funding. AA, HL and AB wrote the manuscript.

### **Declaration of Competing Interest**

The authors declare they have no actual or potential competing financial interests.

### **Acknowledgments**

This work is supported by funding from the European Union's Horizon 2020 research and innovation programme under grant agreement No 953152 (DIAGONAL). The authors would like to thank Simone Ligi from Graphene-XT, Alexis Grigoropoulos from Creative Nano and Gunther Van Kerckhove from OCSiAl Europe Sarl from providing the materials and critically reading the manuscript, Cathy Royer from Plateforme Imagerie In Vitro de l'ITI Neurostra (CNRS UAR 3156, University of Strasbourg) for the sample fixation and TEM observations, and Lucas Jacquemin for his help on XPS analyses.

### **Supporting Information**

Additional information and figures related with this study can be found in Supporting Information.

## References

- (1) Maheswaran, R.; Shanmugavel, B. P. A Critical Review of the Role of Carbon Nanotubes in the Progress of Next-Generation Electronic Applications. *J. Electron. Mater.* **2022**, *51* (6), 2786–2800. <https://doi.org/10.1007/s11664-022-09516-8>.
- (2) Faruque, M. A. Al; Syduzzaman, M.; Sarkar, J.; Bilisik, K.; Naebe, M. A Review on the Production Methods and Applications of Graphene-Based Materials. *Nanomaterials* **2021**, *11* (9). <https://doi.org/10.3390/nano11092414>.
- (3) Lovén, K.; Franzén, S. M.; Isaxon, C.; Messing, M. E.; Martinsson, J.; Gudmundsson, A.; Pagels, J.; Hedmer, M.; Lovén, K.; Franzén, S. M.; Isaxon, C.; Messing, M. E.; Gudmundsson, A.; Hedmer, M. Emissions and Exposures of Graphene Nanomaterials, Titanium Dioxide Nanofibers, and Nanoparticles during down-Stream Industrial Handling. *J. Expo. Sci. Environ. Epidemiol.* **2021**, *31* (4), 736–752. <https://doi.org/10.1038/s41370-020-0241-3>.
- (4) Bergamaschi, E.; Garzaro, G.; Jones, G. W.; Buglisi, M.; Caniglia, M.; Godono, A.; Bosio, D.; Fenoglio, I.; Canu, I. G. Occupational Exposure to Carbon Nanotubes and Carbon Nanofibres: More than a Cobweb. *Nanomaterials* **2021**, *11* (3), 1–15. <https://doi.org/10.3390/nano11030745>.
- (5) Artiga, Á.; Serrano-Sevilla, I.; De Matteis, L.; Mitchell, S. G.; De La Fuente, J. M. Current Status and Future Perspectives of Gold Nanoparticle Vectors for SiRNA Delivery. *J. Mater. Chem. B* **2019**, *7* (6), 876–896. <https://doi.org/10.1039/c8tb02484g>.
- (6) Schinwald, A.; Murphy, F. A.; Jones, A.; MacNee, W.; Donaldson, K. Graphene-Based Nanoplatelets: A New Risk to the Respiratory System as a Consequence of Their Unusual Aerodynamic Properties. *ACS Nano* **2012**, *6* (1), 736–746. <https://doi.org/10.1021/nn204229f>.
- (7) Shao, Y.; Wang, X.; Wang, L.; Huang, Y.; Wei, Q.; Sun, W.; Lai, X.; Yang, F.; Li, F.; Huang, Y. Graphene Quantum Dots Disturbed the Energy Homeostasis by Influencing Lipid Metabolism of Macrophages. *Toxicology* **2023**, *484* (December 2022), 153389. <https://doi.org/10.1016/j.tox.2022.153389>.

- (8) de Luna, L. A. V.; Loret, T.; Fordham, A.; Arshad, A.; Drummond, M.; Dodd, A.; Lozano, N.; Kostarelos, K.; Bussy, C. Lung Recovery from DNA Damage Induced by Graphene Oxide Is Dependent on Size, Dose and Inflammation Profile. *Part. Fibre Toxicol.* **2022**, *19* (1), 1–21. <https://doi.org/10.1186/s12989-022-00502-w>.
- (9) Huang, M.; Xiao, M.; Dong, J.; Huang, Y.; Sun, H.; Wang, D. Synergistic Anti-Inflammatory Effects of Graphene Oxide Quantum Dots and Trans-10-Hydroxy-2-Decenoic Acid on LPS-Stimulated RAW 264.7 Macrophage Cells. *Biomater. Adv.* **2022**, *136* (December 2021), 212774. <https://doi.org/10.1016/j.bioadv.2022.212774>.
- (10) Qin, Y.; Zhou, Z.; Pan, S.; He, Z.; Zhang, X.; Qiu, J.; Duan, W.; Yang, T.; Zhou, S. Inflammatory Response via P38 Mitogen-Activated Protein Kinase and Nuclear Factor- $\kappa$ B Mediated Signaling Pathways in Activated. *Toxicology* **2015**, *327*, 62–76. <https://doi.org/10.1016/j.tox.2014.10.011>.
- (11) Di Ianni, E.; Møller, P.; Vogel, U. B.; Jacobsen, N. R. Pro-Inflammatory Response and Genotoxicity Caused by Clay and Graphene Nanomaterials in A549 and THP-1 Cells. *Mutat. Res. - Genet. Toxicol. Environ. Mutagen.* **2021**, *872* (July 2021). <https://doi.org/10.1016/j.mrgentox.2021.503405>.
- (12) Song, F.; Tang, X.; Zhao, W.; Huang, C.; Dai, X.; Cao, Y. Activation of Kruppel-like Factor 6 by Multi-Walled Carbon Nanotubes in a Diameter-Dependent Manner in THP-1 Macrophages in Vitro and Bronchoalveolar Lavage Cells in Vivo. *Environ. Sci. Nano* **2023**, *10*, 855–865. <https://doi.org/10.1039/d2en00926a>.
- (13) Kong, L.; Yan, G.; Huang, X.; Wu, Y.; Che, X.; Liu, J.; Jia, J. Science of the Total Environment Sequential Exposures of Single Walled Carbon Nanotubes and Heavy Metal Ions to Macrophages Induce Different Cytotoxicity. *Sci. Total Environ.* **2023**, *864* (December 2022), 161059. <https://doi.org/10.1016/j.scitotenv.2022.161059>.
- (14) Bjornson-Hooper, Z. B.; Fragiadakis, G. K.; Spitzer, M. H.; Chen, H.; Madhiredy, D.; Hu, K.; Lundsten, K.; McIlwain, D. R.; Nolan, G. P. A Comprehensive Atlas of Immunological Differences Between Humans, Mice,

- and Non-Human Primates. *Front. Immunol.* **2022**, *13* (March), 1–17.  
<https://doi.org/10.3389/fimmu.2022.867015>.
- (15) Sargeant, T. J.; Fourrier, C. Human Monocyte-Derived Microglia-like Cell Models: A Review of the Benefits, Limitations and Recommendations. *Brain. Behav. Immun.* **2023**, *107* (January 2022), 98–109.  
<https://doi.org/10.1016/j.bbi.2022.09.015>.
- (16) Mukherjee, S. P.; Kostarelos, K.; Fadeel, B. Cytokine Profiling of Primary Human Macrophages Exposed to Endotoxin-Free Graphene Oxide: Size-Independent NLRP3 Inflammasome Activation. *Adv. Healthc. Mater.* **2018**, *7* (4), 1700815. <https://doi.org/10.1002/adhm.201700815>.
- (17) Russier, J.; Treossi, E.; Scarsi, A.; Perrozzi, F.; Dumortier, H.; Ottaviano, L.; Meneghetti, M.; Palermo, V.; Bianco, A. Evidencing the Mask Effect of Graphene Oxide: A Comparative Study on Primary Human and Murine Phagocytic Cells. *Nanoscale* **2013**, *5* (22), 11234–11247.  
<https://doi.org/10.1039/c3nr03543c>.
- (18) Keshavan, S.; Gupta, G.; Martin, S.; Fadeel, B. Multi-Walled Carbon Nanotubes Trigger Lysosome-Dependent Cell Death (Pyroptosis) in Macrophages but Not in Neutrophils. *Nanotoxicology* **2021**, *15* (9), 1125–1150.  
<https://doi.org/10.1080/17435390.2021.1988171>.
- (19) Hannon, G. Endotoxin Contamination of Engineered Nanomaterials : Overcoming the Hurdles Associated with Endotoxin Testing. *WIREs Nanomed Nanobiotechnol.* **2021**, *13* (February), e1738. <https://doi.org/10.1002/wnan.1738>.
- (20) Bermejo-Nogales, A.; Connolly, M.; Rosenkranz, P.; Fernández-Cruz, M. L.; Navas, J. M. Negligible Cytotoxicity Induced by Different Titanium Dioxide Nanoparticles in Fish Cell Lines. *Ecotoxicol. Environ. Saf.* **2017**, *138* (November 2015), 309–319. <https://doi.org/10.1016/j.ecoenv.2016.12.039>.
- (21) Rudolph, J.; Völkl, M.; Jérôme, V.; Scheibel, T.; Freitag, R. Noxic Effects of Polystyrene Microparticles on Murine Macrophages and Epithelial Cells. *Sci. Rep.* **2021**, *11* (1), 1–16. <https://doi.org/10.1038/s41598-021-95073-9>.
- (22) Luanpitpong, S.; Wang, L.; Rojanasakul, Y. The Effects of Carbon Nanotubes on Lung and Dermal Cellular Behaviors. *Nanomedicine* **2014**, *9* (6), 895–912.

<https://doi.org/10.2217/nmm.14.42>.

- (23) Ramos, A. P. *Dynamic Light Scattering Applied to Nanoparticle Characterization*; Elsevier Inc., 2017. <https://doi.org/10.1016/B978-0-323-49778-7/00004-7>.
- (24) Arenas-Guerrero, P.; Delgado, Á. V.; Donovan, K. J.; Scott, K.; Bellini, T.; Mantegazza, F.; Jiménez, M. L. Determination of the Size Distribution of Non-Spherical Nanoparticles by Electric Birefringence-Based Methods. *Sci. Rep.* **2018**, *8* (1), 1–10. <https://doi.org/10.1038/s41598-018-27840-0>.
- (25) Cox, M. C.; Mendes, R.; Silva, F.; Mendes, T. F.; Zelaya-Lazo, A.; Halwachs, K.; Purkal, J. J.; Isidro, I. A.; Félix, A.; Boghaert, E. R.; Brito, C. Application of LDH Assay for Therapeutic Efficacy Evaluation of Ex Vivo Tumor Models. *Sci. Rep.* **2021**, *11* (1), 1–14. <https://doi.org/10.1038/s41598-021-97894-0>.
- (26) Ye, S.; Zhang, H.; Wang, Y.; Jiao, F.; Lin, C.; Zhang, Q. Carboxylated Single-Walled Carbon Nanotubes Induce an Inflammatory Response in Human Primary Monocytes through Oxidative Stress and NF- $\kappa$ B Activation. *J. Nanoparticle Res.* **2011**, *13* (9), 4239–4252. <https://doi.org/10.1007/s11051-011-0368-1>.
- (27) Tabish, T. A.; Zhang, S.; Winyard, P. G. Developing the next Generation of Graphene-Based Platforms for Cancer Therapeutics: The Potential Role of Reactive Oxygen Species. *Redox Biol.* **2018**, *15* (November 2017), 34–40. <https://doi.org/10.1016/j.redox.2017.11.018>.
- (28) Gasser, M.; Wick, P.; Clift, M. J. D.; Blank, F.; Diener, L.; Yan, B.; Gehr, P.; Krug, H. F.; Rothen-Rutishauser, B. Pulmonary Surfactant Coating of Multi-Walled Carbon Nanotubes (MWCNTs) Influences Their Oxidative and pro-Inflammatory Potential in Vitro. *Part. Fibre Toxicol.* **2012**, *9*, 1–13. <https://doi.org/10.1186/1743-8977-9-17>.
- (29) Rennick, J. J.; Johnston, A. P. R.; Parton, R. G. Key Principles and Methods for Studying the Endocytosis of Biological and Nanoparticle Therapeutics. *Nat. Nanotechnol.* **2021**, *16* (3), 266–276. <https://doi.org/10.1038/s41565-021-00858-8>.
- (30) Artiga, Á.; García-Embid, S.; De Matteis, L.; Mitchell, S. G.; de la Fuente, J. M. Effective in Vitro Photokilling by Cell-Adhesive Gold Nanorods. *Front. Chem.*

- 2018**, 6 (June), 234. <https://doi.org/10.3389/fchem.2018.00234>.
- (31) Alfranca, G.; Artiga, Á.; Stepien, G.; Moros, M.; Mitchell, S. G.; de la Fuente, J. M. Gold Nanoprism – Nanorod Face off: Comparing the Heating Efficiency, Cellular Internalization and Thermoablation Capacity. *Nanomedicine (Lond.)* **2016**, 11 (22), 2903–2916. <https://doi.org/10.2217/nmm-2016-0257>.
- (32) Alfranca, G.; Beola, L.; Liu, Y.; Gutiérrez, L.; Zhang, A.; Artiga, A.; Cui, D.; de la Fuente, J. M. In Vivo Comparison of the Biodistribution and Long-Term Fate of Colloids – Gold Nanoprisms and Nanorods – with Minimum Surface Modification. *Nanomedicine* **2019**, 14 (23), 3035–3055. <https://doi.org/10.2217/nmm-2019-0253>.
- (33) Fuoco, C.; Luan, X.; Fusco, L.; Riccio, F.; Giuliani, G.; Lin, H.; Orecchioni, M.; Martín, C.; Cesareni, G.; Feng, X.; Mai, Y.; Bianco, A.; Delogu, L. G. Graphene Nanoribbons Are Internalized by Human Primary Immune Cell Subpopulations Maintaining a Safety Profile: A High-Dimensional Pilot Study by Single-Cell Mass Cytometry. *Appl. Mater. Today* **2022**, 29 (April), 101593. <https://doi.org/10.1016/j.apmt.2022.101593>.
- (34) Orlanducci, S.; Fulgenzi, G.; Margonelli, A.; Rea, G.; Antal, T. K.; Lambreva, M. D. Mapping Single Walled Carbon Nanotubes in Photosynthetic Algae by Single-Cell Confocal Raman Microscopy. *Materials (Basel)*. **2020**, 13 (22), 1–14. <https://doi.org/10.3390/ma13225121>.
- (35) Lin, H.; Ji, D. K.; Lucherelli, M. A.; Reina, G.; Ippolito, S.; Samorì, P.; Bianco, A. Comparative Effects of Graphene and Molybdenum Disulfide on Human Macrophage Toxicity. *Small* **2020**, 16 (35), 1–13. <https://doi.org/10.1002/sml.202002194>.
- (36) Septiadi, D.; Rodriguez-Lorenzo, L.; Balog, S.; Spuch-Calvar, M.; Spiaggia, G.; Taladriz-Blanco, P.; Barosova, H.; Chortarea, S.; Clift, M. J. D.; Teeguarden, J.; Sharma, M.; Petri-Fink, A.; Rothen-Rutishauser, B. Quantification of Carbon Nanotube Doses in Adherent Cell Culture Assays Using UV-VIS-NIR Spectroscopy. *Nanomaterials* **2019**, 9 (12), 1–13. <https://doi.org/10.3390/nano9121765>.
- (37) Kucki, M.; Diener, L.; Bohmer, N.; Hirsch, C.; Krug, H. F.; Palermo, V.; Wick,

- P. Uptake of Label-Free Graphene Oxide by Caco-2 Cells Is Dependent on the Cell Differentiation Status. *J. Nanobiotechnology* **2017**, *15* (1), 1–18.  
<https://doi.org/10.1186/s12951-017-0280-7>.
- (38) Keshavan, S.; Andón, F. T.; Gallud, A.; Chen, W.; Reinert, K.; Tran, L.; Fadeel, B. Profiling of Sub-lethal in Vitro Effects of Multi-walled Carbon Nanotubes Reveals Changes in Chemokines and Chemokine Receptors. *Nanomaterials* **2021**, *11* (4), 883. <https://doi.org/10.3390/nano11040883>.
- (39) Mulens-Arias, V.; Rojas, J. M.; Barber, D. F. The Use of Iron Oxide Nanoparticles to Reprogram Macrophage Responses and the Immunological Tumor Microenvironment. *Front. Immunol.* **2021**, *12* (June).  
<https://doi.org/10.3389/fimmu.2021.693709>.
- (40) Zhang, X.; Luo, M.; Zhang, J.; Yao, Z.; Zhu, J.; Yang, S.; Zhu, Q.; Shen, T. Carbon Nanotubes Promote Alveolar Macrophages toward M2 Polarization Mediated Epithelial-Mesenchymal Transition and Fibroblast-to-Myofibroblast Transdifferentiation. *Nanotoxicology* **2021**, *15* (5), 588–604.  
<https://doi.org/10.1080/17435390.2021.1905098>.
- (41) Mukherjee, S. P.; Bondarenko, O.; Kohonen, P.; Andón, F. T.; Brzicová, T.; Gessner, I.; Mathur, S.; Bottini, M.; Calligari, P.; Stella, L.; Kisin, E.; Shvedova, A.; Autio, R.; Salminen-Mankonen, H.; Lahesmaa, R.; Fadeel, B. Macrophage Sensing of Single-Walled Carbon Nanotubes via Toll-like Receptors. *Sci. Rep.* **2018**, *8* (1), 1–17. <https://doi.org/10.1038/s41598-018-19521-9>.
- (42) Svadlakova, T.; Kolackova, M.; Vankova, R.; Karakale, R.; Malkova, A.; Kulich, P.; Hubatka, F.; Turanek-Knotigova, P.; Kratochvilova, I.; Raska, M.; Krejsek, J.; Turanek, J. Carbon-Based Nanomaterials Increase Reactivity of Primary Monocytes towards Various Bacteria and Modulate Their Differentiation into Macrophages. *Nanomaterials* **2021**, *11* (10), 2510.  
<https://doi.org/10.3390/nano11102510>.
- (43) Fusco, L.; Pelin, M.; Mukherjee, S.; Keshavan, S.; Sosa, S.; Martín, C.; González, V.; Vázquez, E.; Prato, M.; Fadeel, B.; Tubaro, A. Keratinocytes Are Capable of Selectively Sensing Low Amounts of Graphene-Based Materials: Implications for Cutaneous Applications. *Carbon N. Y.* **2020**, *159*, 598–610.

<https://doi.org/10.1016/j.carbon.2019.12.064>.

- (44) Jia, P. P.; Sun, T.; Junaid, M.; Xiong, Y. H.; Wang, Y. Q.; Liu, L.; Pu, S. Y.; Pei, D. S. Chronic Exposure to Graphene Oxide (GO) Induced Inflammation and Differentially Disturbed the Intestinal Microbiota in Zebrafish. *Environ. Sci. Nano* **2019**, *6* (8), 2452–2469. <https://doi.org/10.1039/c9en00364a>.
- (45) Di Ianni, E.; Erdem, J. S.; Møller, P.; Sahlgren, N. M.; Poulsen, S. S.; Knudsen, K. B.; Zienolddiny, S.; Saber, A. T.; Wallin, H.; Vogel, U.; Jacobsen, N. R. In Vitro-in Vivo Correlations of Pulmonary Inflammogenicity and Genotoxicity of MWCNT. *Part. Fibre Toxicol.* **2021**, *18* (1), 1–16. <https://doi.org/10.1186/s12989-021-00413-2>.
- (46) Netkueakul, W.; Korejwo, D.; Hammer, T.; Chortarea, S.; Rupper, P.; Braun, O.; Calame, M.; Rothen-Rutishauser, B.; Buerki-Thurnherr, T.; Wick, P.; Wang, J. Release of Graphene-Related Materials from Epoxy-Based Composites: Characterization, Quantification and Hazard Assessment: In Vitro. *Nanoscale* **2020**, *12* (19), 10703–10722. <https://doi.org/10.1039/c9nr10245k>.
- (47) Brown, A. S.; Hooton, J.; Schaefer, C. A.; Zhang, H.; Petkova, E.; Babulas, V.; Perrin, M.; Gorman, J. M.; Susser, E. S. Elevated Maternal Interleukin-8 Levels and Risk of Schizophrenia in Adult Offspring. *Am. J. Psychiatry* **2004**, *161* (5), 889–895. <https://doi.org/10.1176/appi.ajp.161.5.889>.
- (48) Taub, D. D.; Anver, M.; Oppenheim, J. J.; Longo, D. L.; Murphy, W. J. T Lymphocyte Recruitment by Interleukin-8 (IL-8): IL-8-Induced Degranulation of Neutrophils Releases Potent Chemoattractants for Human T Lymphocytes Both in Vitro and in Vivo. *J. Clin. Invest.* **1996**, *97* (8), 1931–1941. <https://doi.org/10.1172/JCI118625>.
- (49) Lu, Y. J.; Wang, Y. H.; Sahu, R. S.; Chen, J. P.; Dash, B. S.; Chung, P. J.; Yang, H. W.; Chuang, E. Y.; Hwang, T. L. Mechanism of Nanoformulated Graphene Oxide-Mediated Human Neutrophil Activation. *ACS Appl. Mater. Interfaces* **2020**, *12* (36), 40141–40152. <https://doi.org/10.1021/acsami.0c12490>.
- (50) Martín, C.; Ruiz, A.; Keshavan, S.; Reina, G.; Murera, D.; Nishina, Y.; Fadeel, B.; Bianco, A. A Biodegradable Multifunctional Graphene Oxide Platform for Targeted Cancer Therapy. *Adv. Funct. Mater.* **2019**, *29* (39), 1–11.

<https://doi.org/10.1002/adfm.201901761>.

- (51) Martín, C.; Jun, G.; Schurhammer, R.; Reina, G.; Chen, P.; Bianco, A.; Ménard-Moyon, C. Enzymatic Degradation of Graphene Quantum Dots by Human Peroxidases. *Small* **2019**, *15* (52), 1–7. <https://doi.org/10.1002/sml.201905405>.
- (52) Kagan, V. E.; Konduru, N. V.; Feng, W.; Allen, B. L.; Conroy, J.; Volkov, Y.; Vlasova, I. I.; Belikova, N. A.; Yanamala, N.; Kapralov, A.; Tyurina, Y. Y.; Shi, J.; Kisin, E. R.; Murray, A. R.; Franks, J.; Stolz, D.; Gou, P.; Klein-Seetharaman, J.; Fadeel, B.; Star, A.; Shvedova, A. A. Carbon Nanotubes Degraded by Neutrophil Myeloperoxidase Induce Less Pulmonary Inflammation. *Nat. Nanotechnol.* **2010**, *5* (5), 354–359. <https://doi.org/10.1038/nnano.2010.44>.
- (53) Chu, C.; Zhou, L.; Xie, H.; Pei, Z.; Zhang, M.; Wu, M.; Zhang, S.; Wang, L.; Zhao, C.; Shi, L.; Zhang, N.; Niu, Y.; Zheng, Y.; Zhang, R. Pulmonary toxicities from a 90-day chronic inhalation study with carbon black nanoparticles in rats related to the systemical immune effects. *Int J Nanomedicine.* **2019**, *14*, 2995–3013. <https://doi.org/10.2147/IJN.S198376>.
- (54) Lee, J. S.; Shin, J. H.; Choi, B. S. Serum Levels of IL-8 and ICAM-1 as Biomarkers for Progressive Massive Fibrosis in Coal Workers' Pneumoconiosis. *J. Korean Med. Sci.* **2015**, *30* (2), 140–144. <https://doi.org/10.3346/jkms.2015.30.2.140>.